Fabrication and open-loop control of three-lobed nonspherical Janus microrobots

Zameer Hussain Shah, Max Sockolich, David Rivas, Sambeeta Das

Department of Mechanical Engineering, University of Delaware, Newark, DE 19716 USA E-mail: samdas@udel.edu

Abstract. In this study, we propose a simple and efficient method to fabricate three-lobed nonspherical Janus microrobots. These microrobots can be actuated by a harmless magnetic field. Utilizing organosilica as the material of choice, we leverage its versatile silane chemistry to enable various surface modifications and functionalities. The fabricated microrobots demonstrate two distinct modes of motion, making them well-suited for cell transportation and drug delivery tasks. Their unique shape and motion characteristics allow for precise and targeted movement. Integrating these microrobots into therapeutic delivery platforms can revolutionize medical treatments, offering enhanced precision, efficiency, and versatility in delivering therapies to specific sites.

Keywords; microrobots; open-loop control; magnetic; therapeutic delivery

Introduction. Untethered microrobots can deliver therapeutics in a minimally invasive manner [1], accessing otherwise unreachable areas of the human body [2, 3.] The potential applications of these microrobots in biomedicine are extensive, ranging from sensing [4-7], to drug delivery [8-10], and even regenerative medicine [11], etc. In particular, microrobots are highly suitable for cellular applications in regenerative medicine, as they can rapidly penetrate cells and achieve effective intracellular delivery [3]. Cell-based therapies, which aim to restore damaged or diseased tissues and organs [12] require precise transportation of cells to the targeted locations for transplantation [13, 14]. Any failure in cell delivery could result in a serious immune response [15]. Therefore, it is crucial to ensure accurate and noninvasive delivery of cells, where microrobots can play a vital role [16].

In recent years, the field of microrobotics has developed rapidly after the pioneering work reported by Ozin[17, 18], Sen[19, 20], and Mallouk[21, 22]. In particular, there have been several reports of microrobots transporting cells. Balasubramanian et al. [23] developed microengine rockets coated with antibodies that bind to antigens expressed by cancer cells. This approach allowed for the cells to be transported along a preselected path. Similarly, Gao et al. utilized a similar method for the transportation of circulating tumor cells [24]. Likewise, Sanchez et al. [25] developed chemically propelled microrobots that could be controlled magnetically, allowing for the selective loading, transportation, and delivery of multiple cells to specific locations in a fluid. However, all of the above-mentioned studies are based on chemically powered microrobots, which require high concentrations of toxic chemical fuel that can harm living cells [26]. As an alternative, magnetically actuated microbots have been developed for biological applications [27]. In the last decade, various research groups have developed magnetically actuated microrobots for cell delivery. Most of these microrobots were fabricated using direct laser writing or other sophisticated manufacturing technologies [28] which are not readily available to the wider research community.

Colloidal synthesis presents a simple and scalable fabrication technique that could be utilized for commercial production [29]. The initial investigations into microrobots have greatly benefited from colloidal synthesis, with a majority of synthesized microrobots being Janus colloids with spherical shapes [30]. While spherical Janus microrobots are promising for fundamental research [31], nonspherical Janus microrobots are highly preferred for practical applications [32]. However, the fabrication of non-spherical microrobots via colloidal synthesis is rare, primarily due to the difficulty in manufacturing such particles.

In the current work, we report the fabrication of three-lobed nonspherical Janus microrobots by using a bench-top colloidal synthesis route. The particles were coated with a nickel layer for a sharp magnetic response, thus giving them a nonspherical Janus characteristic. We demonstrate that these microrobots could be moved to a desired location by controlling them with a rotating magnetic field. Due to their unique shape, they offer promising cargo-carrying opportunities.

Magnetic setup. Our experimental setup utilizes an electromagnetic manipulation system with rotating homogeneous magnetic fields. A Helmholtz coil system composed of six rings, assembled into three pairs, is optimized to achieve this. The coils are made of copper wires wrapped around the rings of three different sizes - small, medium, and large - and mounted on an inverted microscope. The medium and large coils are vertically mounted, while the small coils are horizontally mounted to avoid interference with the objective turret or condenser lens. The platform's dimensions are approximately 230 mm in length and 140 mm in width. Our design enables precise control of the rotating magnetic fields, making it easier to manipulate biological samples during experiments. The magnetic setup components, including the platform, slide arm, and coils, were 3D printed with PLA on an Ender 3 Pro machine. After applying a 1 A current, a uniform magnetic field of 2 mT for each of the medium and large ring pairs and 4 mT for the small ring pair was generated. The coils were connected to a motherboard for power and controlled wirelessly by a tablet computer connected to an X-box joystick, as shown in Fig. 1b. This setup allowed for precise control of the magnetic field direction during microrobotic manipulation.

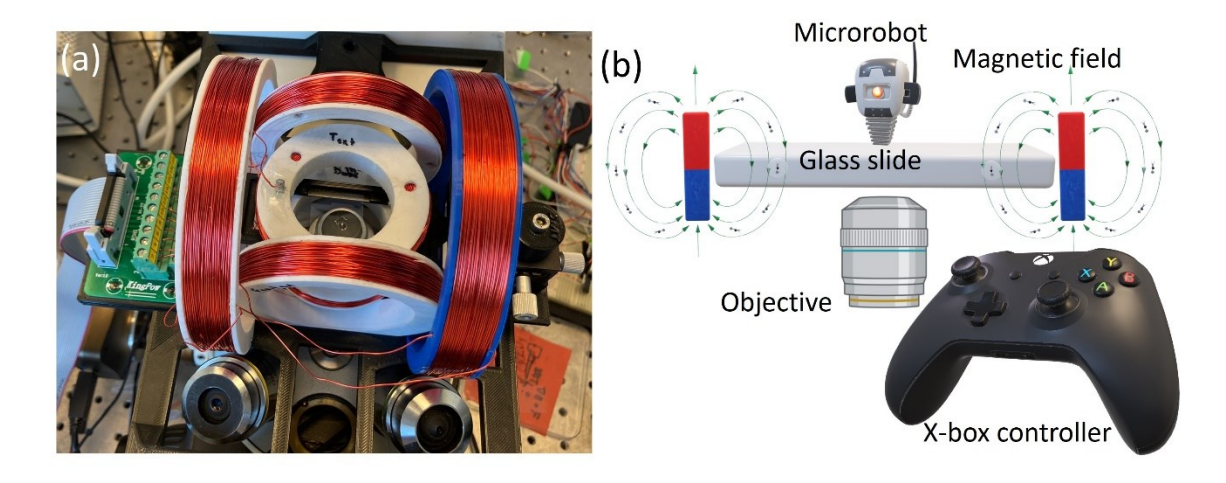


Fig. 1. Magnetic setup for the microrobot control. (a) Helmholtz coils mounted on an inverted microscope and (b) a schematic of microrobotic control employed in this study.

Our team developed a Python-based graphical user interface using Tkinter and Gpiozero libraries. This user-friendly interface can accurately control the current in each coil, allowing for the application of constant magnetic fields in a user-defined direction. The user inputs the desired magnetic field direction and strength, which are converted into their corresponding x and y components. The current sent through the x and y coils is then adjusted proportionally to achieve the desired magnetic field strength. To enhance field strength, the software simultaneously sends an opposite polarity signal to the oppositely facing coil. The device is controlled via a wireless USB gaming controller, with the left joystick used for 360° orientation control and the right joystick for adjusting the magnetic field direction of a rolling microrobot.

The rotating magnetic field can be generated in any user-defined direction by applying a time-varying sine wave to each of the X, Y, and Z-axis coils using following equations.

$$Bx = A[\cos(\gamma)\cos(\alpha)\cos(\omega t) + \sin(\alpha)\sin(\omega t)]$$
 (1)

$$By = -A[\cos(\gamma)\sin(\alpha)\cos(\omega t) + (\cos(\alpha)\sin(\omega t)]$$
 (2)

$$Bz = A\sin(\gamma)\cos(\omega t) \tag{3}$$

where γ is the azimuthal angle from the Z-axis, α is the polar angle from the Y-axis, A is the magnetic field magnitude, and ω is the frequency that controls the speed of the rolling microrobot. By default, an azimuthal angle of 90° was set, and the polar angle could be adjusted to steer the direction of the rolling microrobot.

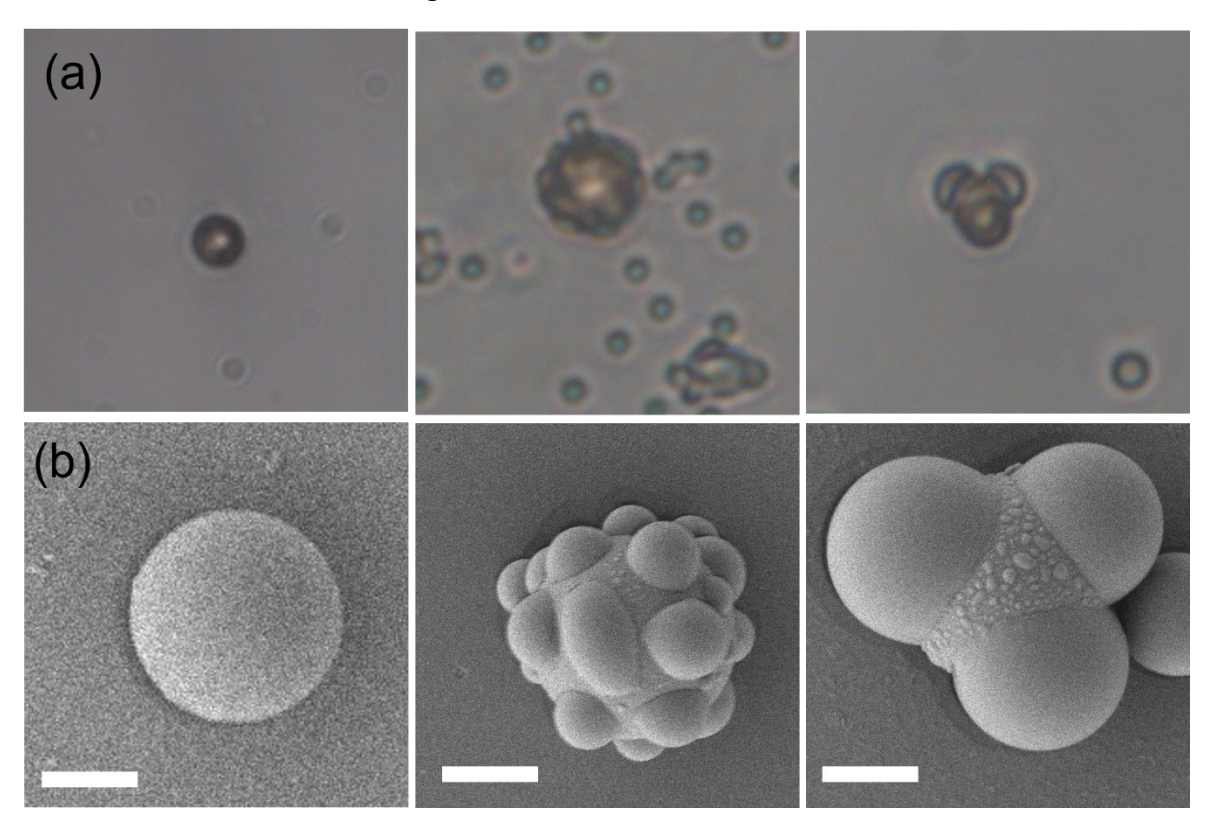


Fig. 2. Synthesis of three-lobed nonspherical Janus microrobots. (a) Optical images (i) magnetic seed particles, (ii) heterogeneous nucleation of oil on the seeds, (iii) growth of droplets to achieve a three-lobed shape, and (b) corresponding SEM images captured at different synthesis stages. Scale bars in (b) are $2 \mu m$.

We optimized the magnetic setup for microrobotic manipulation and investigated the motion of our nonspherical Janus microrobots. We synthesized these microrobots using a modified procedure developed by Sacanna et al. [33], where we used magnetic polystyrene microspheres as seed particles for the heterogeneous nucleation of a polymerizable oil (TPM) onto them. (Synthesis procedure is given in the supplementary information). We employed sonication to ensure most of the particles were singlets and then rapidly injected hTPM into the solution. Under basic conditions, TPM undergoes hydrolysis and deprotonation, resulting in the formation of organosilica [34]. The clear suspension turned milky-white within a few minutes of injection. Heterogeneous nucleation of silica onto the seed particles was observed under an optical microscope until the desired morphology was achieved. Optical bright field and SEM images are provided in Fig. 2.

Results and Discussions.

When a microparticle with an embedded magnetic component is placed in a magnetic field, it experiences a magnetic force \vec{F} given by:

$$\overrightarrow{F} = (\overrightarrow{m}. \nabla) \overrightarrow{B} \tag{4}$$

Where \vec{B} is the magnetic field and \vec{m} is the magnetization or the magnetic moment of the particle. The particle also experiences a magnetic torque $\vec{\tau}$ which can be predicted from the following equation:

$$\vec{\tau} = \vec{m} \times \vec{B} \tag{5}$$

When the magnetic field is turned on, the magnetic moment of the particles aligns itself with the external magnetic field. By changing the direction of the applied magnetic field, the magnetic moment alignment also changes which offers a fundamental tool to control motion at the nanoscale. Equation 5 implies that by rotating the applied magnetic field in a certain direction by a certain angle will rotate a magnetized particle until the magnetic moment is aligned with the new direction of the magnetic field [35].

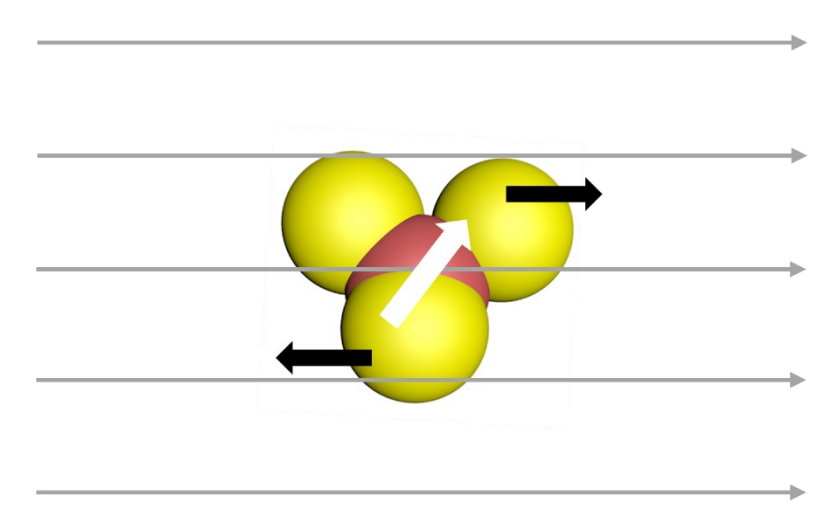


Fig. 3. Schematic of rolling motion of three-lobed nonspherical Janus microrobots in a rotating magnetic field. The white arrow shows the magnetic moment of the microrobots.

In order to manipulate the three-lobed nonspherical Janus microrobots, we utilized a rotating magnetic field. It was observed that these microrobots were inactive in the absence of a magnetic field. However, once the magnetic field was turned on, the microrobots aligned themselves with the applied magnetic field. By controlling the direction of the magnetic field using an X-box controller, we were able to move the microrobots in the desired directions. This rolling motion of the mickey mouse shaped microrobots is depicted schematically in Fig. 3.

It is interesting to note that the seed particles used for the fabrication of these microrobots are magnetic, which allows for the microrobots to respond to the magnetic field without any additional metal coating. However, we found that the response was much weaker for the uncoated particles. This may be due to the increased weight of the microrobots as a result of the three large organosilica lobes. In contrast, the nickel-coated particles showed a sharp response to the rotating magnetic field (as shown in Fig. 4a and video S1). Therefore, we performed all experiments on the nickel-coated microrobots.

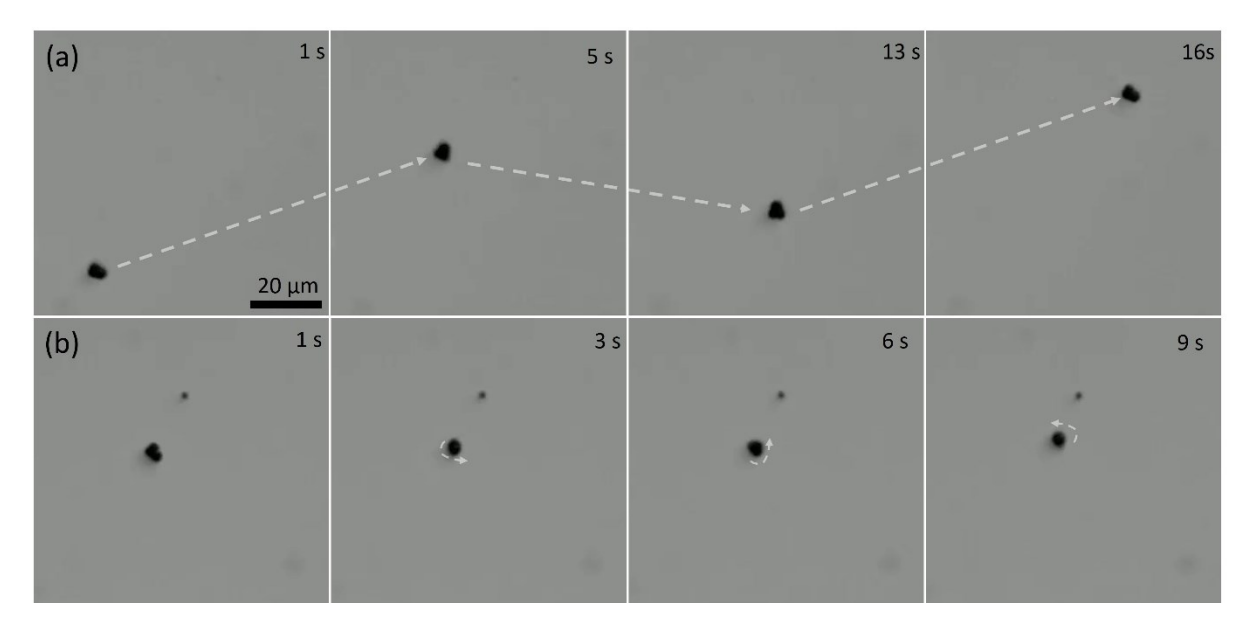


Fig. 4. Motion of three-lobed nonspherical Janus microrobots in a rotating magnetic field. (a) Time-lapse images of translational motion and (b) time-lapse images of a microrobot at different stages of rotational motion.

In the absence of a magnetic field, the three-lobed nonspherical Janus microrobots displayed Brownian motion. However, the microrobots exhibited a clear response as soon as the magnetic field was applied. The magnetic moment of the microrobots aligned themselves to the magnetic field, which was captured and recorded by a microscope-attached camera. Video S1 and Fig. 4a demonstrate the magnetic response of the microrobots.

We used a rotating magnetic field and an Xbox controller to move the microrobots in the desired direction. By changing the direction of the magnetic field, the microrobots were moved in different directions. The microrobots were moved towards the upper right corner of the screen (Fig. 4a, 5 s), bottom right corner (Fig. 4a, 13 s), and upper left corner (Fig. 4a, 16 s) at a frequency of 2 Hz. The motion experiments of these microrobots were conducted at this frequency.

Apart from the translational motion, the microrobots also demonstrated a rotational motion along a fixed axis, which was achieved by changing the angle of the applied magnetic field. The rotational motion is displayed in Fig. 4b and video S2.

To ensure the reliability and reproducibility of our experimental results, we took several measures. First, we carefully optimized the magnetic setup for microrobotic manipulation, considering factors such as the strength and directionality of the magnetic field. We thoroughly calibrated our instruments and equipment to minimize any potential sources of error. Furthermore, we conducted multiple replicates of our experiments to assess the consistency of the observed phenomena. We found that both the chemical synthesis of the three-lobed microrobots and their magnetic manipulation was highly reproducible.

Conclusions. In conclusion, we have successfully produced three-lobed nonspherical Janus microrobots that can be controlled by a magnetic field, exhibiting both translational and rotational motion. This was achieved through a process of heterogeneous nucleation and polymerization of organosilica precursor onto commercially available magnetic polystyrene microspheres. The unique shape and movement of these microrobots make them an exciting prospect for applications in therapeutic delivery. For example, by attaching or encapsulating

cells onto the surface of the microrobots, they can transport cells to desired locations within the body. This can be particularly useful in regenerative medicine and tissue engineering, where the precise placement of cells is crucial for successful tissue repair or organ regeneration. We are currently exploring the potential of these microrobots for drug and cell delivery purposes.

Acknowledgment. This work is supported by an Institutional Development Award (IDeA) from the NIGMS of the National Institutes of Health under grant number U54-GM104941, from the NIGMS of the National Institute of Health under grant number 1R35GM147451, from the National Science Foundation under grant number 2020973 and under grant number 2218980.

References

- B. J. Nelson, I. K. Kaliakatsos, and J. J. Abbott, Annual Review of Biomedical Engineering **12**, 55 (2010).
- J. Choi, J. Hwang, J.-y. Kim, and H. Choi, Advanced Healthcare Materials 10, 2001596 (2021).
- P. L. Venugopalan, B. Esteban-Fernández de Ávila, M. Pal, A. Ghosh, and J. Wang, ACS Nano 14, 9423 (2020).
- ⁴ A. K. Shukla, S. Bhandari, and K. K. Dey, Materials Today Communications **28**, 102504 (2021).
- M. Sitti, H. Ceylan, W. Hu, J. Giltinan, M. Turan, S. Yim, and E. Diller, Proceedings of the IEEE **103**, 205 (2015).
- R. Maria-Hormigos, B. Jurado-Sánchez, and A. Escarpa, Analytical and Bioanalytical Chemistry **414**, 7035 (2022).
- A. K. Shukla, D. Bhatia, and K. K. Dey, ACS Applied Nano Materials **6**, 8017 (2023).
- X. Song, et al., Advanced Materials **34**, 2204791 (2022).
- ⁹ S. Park and G. Yossifon, ACS Sensors **5**, 936 (2020).
- M. Luo, Y. Feng, T. Wang, and J. Guan, Advanced Functional Materials **28**, 1706100 (2018).
- ¹¹ J. Li, et al., Science Robotics **3**, eaat8829 (2018).
- A. S. Mao and D. J. Mooney, Proceedings of the National Academy of Sciences of the United States of America **112**, 14452 (2015).
- D. M. Hoang, et al., Signal Transduction and Targeted Therapy 7, 272 (2022).
- N. H. Yu, et al., Tissue engineering and regenerative medicine **15**, 639 (2018).
- P. A. Beachy, S. S. Karhadkar, and D. M. Berman, Nature **432**, 324 (2004).
- W. Chen, H. Zhou, B. Zhang, Q. Cao, B. Wang, and X. Ma, Advanced Functional Materials **32**, 2110625 (2022).
- G. A. Ozin, I. Manners, S. Fournier-Bidoz, and A. Arsenault, Advanced Materials 17, 3011 (2005).
- S. Fournier-Bidoz, A. C. Arsenault, I. Manners, and G. A. Ozin, Chemical Communications, 441 (2005).
- W. F. Paxton, A. Sen, and T. E. Mallouk, Chemistry A European Journal 11, 6462 (2005).
- ²⁰ T. R. Kline, W. F. Paxton, T. E. Mallouk, and A. Sen, Angew Chem Intl Ed **44**, 744 (2005).

- W. F. Paxton, K. C. Kistler, C. C. Olmeda, A. Sen, S. K. St. Angelo, Y. Cao, T. E. Mallouk, P. E. Lammert, and V. H. Crespi, J Am Chem Soc 126, 13424 (2004).
- W. F. Paxton, S. Sundararajan, T. E. Mallouk, and A. Sen, Angew Chem Intl Ed 45, 5420 (2006).
- S. Balasubramanian, et al., Angew Chem Intl Ed **50**, 4161 (2011).
- ²⁴ W. Gao and O. C. Farokhzad, Angew Chem Intl Ed **50**, 7220 (2011).
- S. Sanchez, A. A. Solovev, S. Schulze, and O. G. Schmidt, Chemical Communications 47, 698 (2011).
- ²⁶ S. Sánchez, L. Soler, and J. Katuri, Angew. Chem. Int. Ed. **54**, 1414 (2015).
- ²⁷ M. Sitti and D. S. Wiersma, Advanced Materials **32**, 1906766 (2020).
- J. Li and M. Pumera, Chemical Society Reviews **50**, 2794 (2021).
- Y. Pu, F. Cai, D. Wang, J.-X. Wang, and J.-F. Chen, Industrial & Engineering Chemistry Research **57**, 1790 (2018).
- ³⁰ Q. Chen, J. Yan, J. Zhang, S. C. Bae, and S. Granick, Langmuir **28**, 13555 (2012).
- B. Jurado-Sánchez, M. Pacheco, R. Maria-Hormigos, and A. Escarpa, Applied Materials Today 9, 407 (2017).
- A. Sahari, D. Headen, and B. Behkam, in 2012 Annual International Conference of the IEEE Engineering in Medicine and Biology Society, p. 6580 (2012).
- S. Sacanna, M. Korpics, K. Rodriguez, L. Colón-Meléndez, S.-H. Kim, D. J. Pine, and G.-R. Yi, Nat. Commun. 4, 1688 (2013).
- C. van der Wel, R. K. Bhan, R. W. Verweij, H. C. Frijters, Z. Gong, A. D. Hollingsworth, S. Sacanna, and D. J. Kraft, Langmuir **33**, 8174 (2017).
- M. T. Hou, H.-M. Shen, G.-L. Jiang, C.-N. Lu, I.-J. Hsu, and J. A. Yeh, Applied Physics Letters 96, 024102 (2010).